



ELSEVIER

Contents lists available at ScienceDirect

Organic Electronics

journal homepage: www.elsevier.com/locate/orgel

Charge carrier mobility and lifetime of organic bulk heterojunctions analyzed by impedance spectroscopy

Germà Garcia-Belmonte^{a,*}, Antoni Munar^a, Eva M. Barea^a, Juan Bisquert^a, Irati Ugarte^b, Roberto Pacios^b

^a *Departament de Física, Universitat Jaume I, 12071 Castelló, Spain*

^b *Department of Microsystems, IKERLAN-IK4 S. Coop., P^o J.M. Arizmendiarieta, 2, 20500 Arrasate-Mondragón, Gipuzkoa, Spain*

ARTICLE INFO

Article history:

Received 24 April 2008

Received in revised form 4 June 2008

Accepted 8 June 2008

Available online 17 June 2008

PACS:

73.40.Ei

73.40.Lq

73.61.Wp

84.60.Jt

Keywords:

P3HT:PCBM heterojunctions

Organic solar cells

Capacitance

Impedance spectroscopy

Mobility

Lifetime

ABSTRACT

Charge carrier diffusion and recombination in an absorber blend of poly(3-hexylthiophene) (P3HT) and [6,6]-phenyl C₆₁-butyric acid methyl ester (PCBM) with indium tin oxide (ITO) and aluminium contacts have been analyzed in the dark by means of impedance spectroscopy. Reverse bias capacitance exhibits Mott–Schottky-like behavior indicating the formation of a Schottky junction (band bending) at the P3HT:PCBM–Al contact. Impedance measurements show that minority carrier (electrons) diffuse out of the P3HT:PCBM–Al depletion zone and their accumulation contributes to the capacitive response at forward bias. A diffusion–recombination impedance model accounting for the mobility and lifetime parameters is outlined. Electron mobility results to be $2 \times 10^{-3} \text{ cm}^2 \text{ V}^{-1} \text{ s}^{-1}$ and lifetime lies within the milliseconds timescale.

© 2008 Elsevier B.V. All rights reserved.

1. Introduction

Organic conducting materials are at the heart of bulk heterojunction (BHJ) solar cells, a promising alternative to silicon-based solar cells due to their optical, electronic and mechanical properties [1]. Bulk heterojunctions are formed by an interpenetrating blend of an optically active polymer and electron accepting molecules. At the optically active polymer excitons are created by light absorption. This exciton dissociates at the polymer/molecule interface, thus spatially separating the electrons and holes which therefore can be transported to the electrodes by hopping.

When using derivatives of poly(phenylene vinylene) (PPV) as hole transporting material (HTM), some aspects of the BHJ device operation (particularly the internal electric field distribution [2] and the transport mechanisms [3,4]) have been properly interpreted. Blends formed of PPV derivatives and fullerenes are considered to form undoped systems. Therefore, the basic device model resembles that proposed for a-Si thin film p–i–n structures [3]. Transport is mainly determined by charge carrier drift upon the electrical field driving force. Recently, BHJ organic solar cells using P3HT as HTM have shown high performance [5]. P3HT exhibits relatively high hole mobility ($\sim 10^{-4}$ – $10^{-3} \text{ cm}^2 \text{ V}^{-1} \text{ s}^{-1}$) [6] and can easily undergo p-doping when exposed to the air or moisture [7,8], with the consequent formation of Schottky contacts.

* Corresponding author. Tel.: +34 964 728040; fax: +34 964 729218.
E-mail address: garcia@uji.es (G. Garcia-Belmonte).

Models which regard polymer semiconductors as undoped materials should be then revised to include the effect of band bending (depletion zones) and minority carrier injection and storage in the diode bulk.

The central magnitude that informs about carrier accumulation is the capacitance, which can be readily determined by impedance spectroscopy. This is because in all solar cells the generation of positive and negative carriers creates a splitting of Fermi levels that is ultimately responsible for the photovoltage [9]. In silicon solar cells, for instance, the capacitance shows two main components as a function of the bias [10,11]: a Mott–Schottky characteristic, due to the modulation of the Schottky barrier, at reverse and moderate forward bias, and a chemical capacitance [9], that increases exponentially for intense forward bias. The first characteristic indicates the presence of doping whereby the solar cell device is able to accumulate substantial minorities. Such carrier storage is manifest in the second characteristic, the chemical capacitance, which directly reflects the carrier statistics [9]. In standard dye-sensitized solar cells (DSC) based on nanostructured TiO_2 , the shape of the voltage dependence of the capacitance is somewhat different, since the “hole conductor” is a liquid electrolyte with high ionic concentration, so that the Schottky barrier in the active semiconductor layer is not found. However, the chemical capacitance is very clearly observed and shows the density of states of electrons accumulated in the electron-transporting material (TiO_2) [12,13]. The identification of the voltage-dependent capacitance has become then a major tool for assessing the energetics in a DSC [14] and for interpreting the recombination lifetime [15]. The strong accumulation associated with the unconstrained rise of the Fermi level with bias appears in high performance solar cells [13], while in many other cases, the charge storage is inhibited by additional mechanisms and the solar cell capacitance may become negative at strong forward bias [10].

Given the general significance of the capacitance for interpretation of the fundamental transport and recombination mechanism governing the operation of new classes of solar cell devices, in this paper we present direct measurements and interpretation of the capacitance under reverse and forward voltages of a BHJ structure of the type ITO/PEDOT:PSS/P3HT:PCBM/Al. Reverse bias capacitance exhibits Mott–Schottky-like behavior signaling the formation of a Schottky junction (band bending) at the P3HT:PCBM–Al contact. Impedance modeling allows to extract both the recombination time and mobility of the minority carriers (electrons) at forward bias in the dark.

2. Experimental

We have built diodes with structure ITO/PEDOT:PSS/P3HT:PCBM/Al following the next procedure: RR-P3HT from Rieke Materials and PCBM from Nano-c were dissolved in xylene in a weight ratio of (1:0.75). The solution was heat up to 65 °C and continuously stirred for 3 h. In parallel, ITO substrates from Diamond Coatings with a sheet resistance of 40 Ω/\square were cleaned in 5 min subse-

quent ultrasonic baths of acetone, methanol and isopropanol. They were later introduced in oxygen plasma for 5 min. Baytron P CH8000 from HC Starck was spin-coated on top of the ITO substrate giving a film thickness of ~ 50 nm. The resulting film was annealed at 120 °C for 5 min in order to remove any possible water residual on the film. The P3HT:PCBM film was then spin-cast from the previously prepared solution at 800 rpm. The active layer thickness was measured to be $L \sim 200$ nm. The film was pre-annealed at 85 °C for 5 min to remove any solvent remaining on the film after deposition. Samples were then taken to a vacuum chamber to thermally evaporate the aluminium contacts through a shadow mask. The evaporation was done at $\sim 3 \times 10^{-6}$ atm at rates between 2 and 10 $\text{\AA}/\text{s}$. The active area of the diode, given by the overlap between ITO and aluminium, is 9 mm^2 . The finalized devices were immediately encapsulated with an epoxy resin

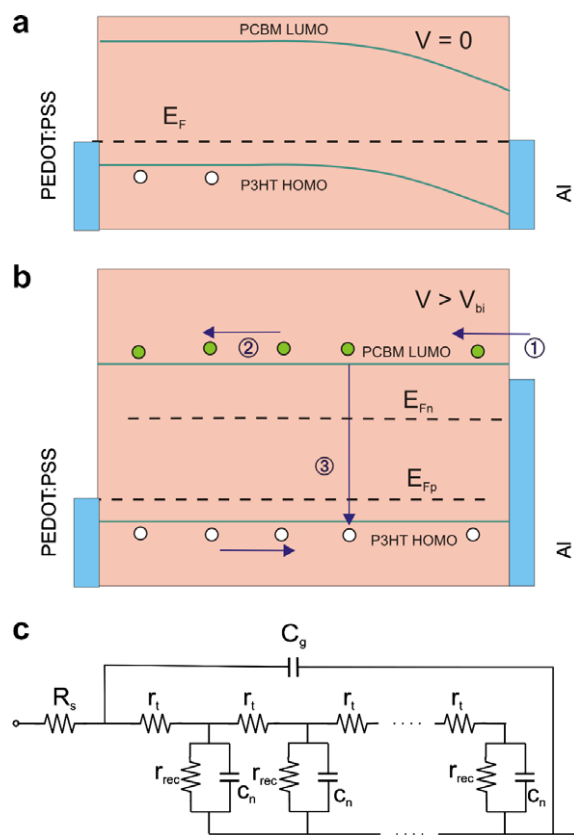


Fig. 1. (a) Band structure of the P3HT:PCBM heterojunction in equilibrium ($V=0$). Band bending appears near the cathode and holes can occupy HOMO states of the P3HT within the neutral region. (b) Main dynamic processes occurring in the diode bulk layer for $V > V_{bi}$. Holes (majority carriers) are able to occupy the whole active layer. Electrons (minority carriers) are injected (1) into the LUMO of the PCBM, diffuse along the diode bulk (2), and eventually recombine with holes (3). (c) Equivalent circuit accounting for the diffusion–recombination mechanism used for fitting. Modulation of stored excess minority carriers gives rise to distributed chemical capacitances C_n . Bimolecular recombination of conduction band electrons and valence band holes are modeled by resistive elements r_{rec} . Transport of electrons is represented by means of r_t . An additional series resistance is needed to model contact and wire effects, R_s . Finally a capacitor $C_g \approx \epsilon \epsilon_0 A/L$ represents dielectric contribution of the diode.

and glass. Even though encapsulation took place right after evaporation, it has to be stressed that devices were briefly in contact with air. Nevertheless, repetitive measurements of dark J - V characteristics (inset of Fig. 2a) gave identical results over several weeks. The impedance measurements were carried out in the air and room temperature, using an Autolab PGSTAT-30 equipped with a frequency analyzer module in the frequency range between 1 MHz and 1 Hz. Ac oscillating amplitude was as low as 10 mV (rms) in order to maintain the linearity of the response.

3. Results and discussion

It is well-known that P3HT is a conjugated polymer that in exposure to oxygen and/or moisture results p-doped [7,8]. Under such conditions, it has been suggested that the P3HT-Aluminum contact shows a Schottky diode behavior. Band bending with a corresponding depletion zone is formed at the contact as indicated in Fig. 1a [16,17]. For a Schottky diode [18] the junction capacitance, which appears as a consequence of the modulation of the depletion layer, exhibits a bias dependence according to the Mott-Schottky relation

$$C^{-2} = \frac{2(V_{\text{bi}} - V)}{A^2 e \epsilon \epsilon_0 N_A} \quad (1)$$

where V_{bi} is the built-in potential, V is the applied voltage, A corresponds to the device active surface (9 mm^2), e accounts for the elementary charge, ϵ is the relative dielectric constant, ϵ_0 the permittivity of the vacuum, and N_A the concentration of acceptor impurities. Our experimental results follow Eq. (1) (Mott-Schottky curve) which exhibits a straight line over a wide bias voltage range (Fig. 2a) yielding $V_{\text{bi}} = 0.43 \text{ V}$ and $N_A = 3.5 \times 10^{16} \text{ cm}^{-3}$, assuming $\epsilon = 3$ for P3HT:PCBM. In this case the depletion region for a reverse bias voltage between 0 and 1 V results to be varying between 63 and 115 nm, compatible with an active layer thickness of 200 nm. At $V = V_{\text{bi}}$ (flat-band conditions) the depletion layer adjacent to the P3HT:PCBM/Al contact disappears and the neutral, doped region extends along the whole diode bulk (Fig. 1b).

As commented in the Introduction, when the Schottky barrier vanishes at $V > V_{\text{bi}}$ it is expected that the device capacitance is governed by a chemical capacitance due to the excess minority carriers C_μ [11,19,20], that is related to the change of the occupancy of electrons in the LUMO of the PCBM, as follows

$$C_\mu = e^2 \frac{dn}{dE_{\text{Fn}}} \quad (2)$$

Here the capacitance is given per unit volume, n corresponds to the electron concentration, and E_{Fn} accounts for the electron quasi-Fermi level (see Fig. 1b). According to Eq. (2), the capacitance should increase as a function of forward bias. For ideal statistics, the increase is exponential [10]. However, it has been shown in classic Schottky diodes [21] that under moderate to large forward bias conditions, minority carrier injection can be limited depending on the barrier heights at the metal-semiconductor junction. Oxidation of the aluminium cathode (due to the preparation conditions) leads to the formation of an Al_2O_3 layer between the aluminium and the P3HT:PCBM. Electron injection from aluminium to PCBM might be blocked to some extent by this tunneling barrier, and could limit charge collection under illumination. This injection-limiting effect yields a peak in the capacitance-voltage characteristics, and eventually a strong negative capacitance component [21].

Fig. 2b shows the measured capacitance at low frequency (100 Hz) as a function of the bias. The capacitance increases in the forward direction, reaching a peak for voltages of approximately 0.6–0.7 V. At this point the capacitance decreases caused by the limitation upon the concentration of minority carriers in the neutral regions of the device. Alternative explanations of a large low-frequency capacitance at forward bias point to the occurrence of charge blocking caused by slow injection/extraction at the contacts [22]. Although these effects cannot be completely discarded, such interpretations are however based on increasing capacitance values at forward bias in opposition to our observations in Fig. 2.

Fig. 3 displays the measured electrical impedance in the complex plane for different forward bias voltages from 0.5 to 1 V. It can be seen that the impedance spectra are com-

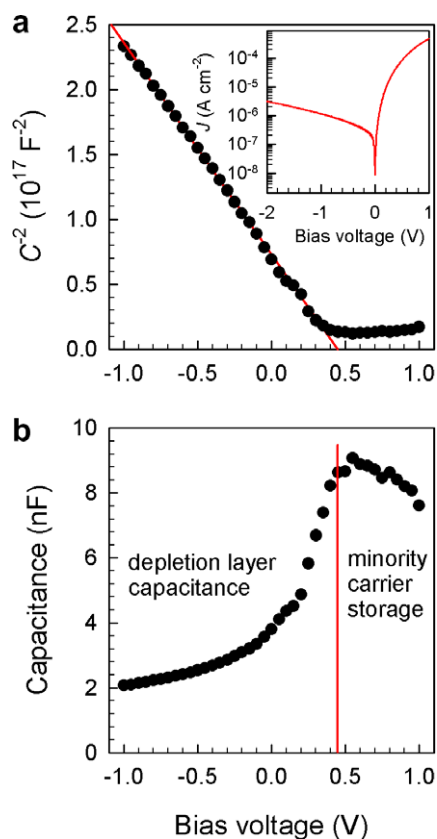


Fig. 2. (a) Mott-Schottky curve (100 Hz) which exhibits a straight line yielding $V_{\text{bi}} = 0.43 \text{ V}$ and $N_A = 3.5 \times 10^{16} \text{ cm}^{-3}$, assuming $\epsilon = 3$ for P3HT:PCBM. In the inset: J - V characteristics measured in the dark. (b) Capacitance (100 Hz) as a function of bias. Vertical line separates voltage regions for which capacitance is determined either by the depletion layer modulation ($V < V_{\text{bi}}$) or the storage of minority carriers ($V > V_{\text{bi}}$).

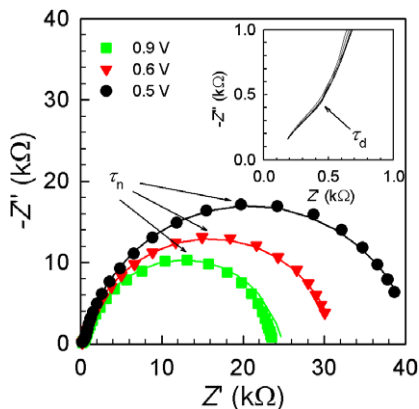


Fig. 3. Impedance spectra measured in the dark at different bias as indicated. Experimental points and fitting results (solid line) using the equivalent circuit model of Fig. 1c. Characteristic times are marked. Inset: detail of the high-frequency interval which signals the transition between diffusion and recombination responses.

posed of a large semicircle at low frequencies together with an almost straight line in the high-frequency part (inset of Fig. 3), which is rather independent of the applied voltage. This type of impedance pattern belongs to the responses usually encountered in systems in which carrier transport is determined by diffusion–recombination between non-absorbing contacts [23]. Injected minority carriers (electrons) from the Al contact are able to diffuse within the bulk neutral region eventually reaching the PEDOT:PSS film which acts as selective contact. Transmission line models able to represent such diffusion–recombination impedance response are well-known [23,24], and have been integrated in standard software. The impedance model (Fig. 1c) consists of an equivalent circuit which comprises distributed resistors r_t , standing for the electron transport, the distributed chemical capacitance $c_n = C_\mu$ and r_{rec} accounting for the electron recombination resistance. An additional series resistance is needed to model contact and wire effects, R_s . Finally a capacitor $C_g \approx \epsilon\epsilon_0 A/L$ represents dielectric contribution of the diode. The impedance model described contains two characteristic times related to the electron diffusion $\tau_d = r_t c_n$ (transit time), and the effective lifetime $\tau_n = r_{rec} c_n$, respectively [23].

By examining Fig. 3 one can observe that fitting curves match the impedance spectra in the whole measuring frequencies. The position of the characteristic times is marked in Fig. 3. $R_s \approx 100 \Omega$, and $C_g \approx 1.0$ nF in agreement with the permittivity value assumed. The electron diffusivity (chemical diffusion coefficient) can be calculated by means of the relation [23]

$$D_n = \frac{L^2}{\tau_d} \quad (3)$$

Here $L = 200$ nm is the thickness of the diffusion layer. Assuming that the electron statistics slightly departs from dilute concentration conditions, the electron mobility might be readily calculated by using the Nernst–Einstein relationship as $\mu_n = eD_n/k_B T$ (being $k_B T$ the thermal energy) [25,26]. Results are summarized in Fig. 4. The electron

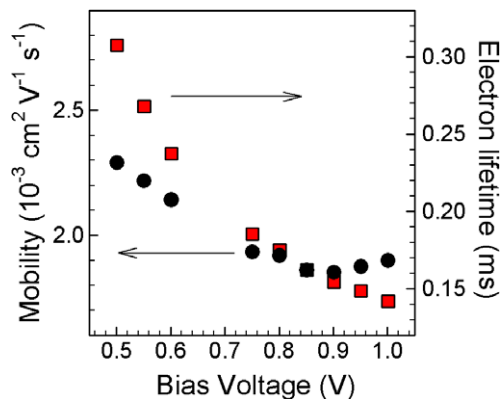


Fig. 4. Electron mobility determined from fitting parameters, using Eq. (3) and the approximation $\mu_n = eD_n/k_B T$. Electron recombination time (effective lifetime) resulting from fits.

mobility extracted from fits exhibits a nearly constant value approximately equal to $2 \times 10^{-3} \text{ cm}^2 \text{ V}^{-1} \text{ s}^{-1}$. This value is in good agreement with that derived using PCBM electron-only devices from J – V measurements, for which current is considered space-charge-limited, and hence electrical field-driven rather than diffusion-determined [27]. Electron effective lifetime results within the time interval 0.3–0.1 ms, decreasing as the bias increases. Such time presumably refers to losses produced by electron–hole bimolecular recombination along the absorber layer, although surface recombination routes cannot be excluded. Alternative methods to investigate charge carrier lifetime such as photoinduced absorption [28,29] find values of similar order.

4. Conclusion

In summary, it has been shown that the P3HT:PCBM–Al contacts show a behavior consistent with a Schottky diode in the dark and under reverse bias. Furthermore, the capacitance values at forward bias are viewed as a strong indication that minority charge carriers play a significant role. With such assumption and measuring ac electrical impedance spectra we propose a model to interpret the diffusion and recombination processes which allows us to determine both the diffusion and recombination time constants. Electron mobility and effective lifetime can therefore be easily computed which permits to reach a deeper understanding of the mechanisms governing doped BHJ devices.

Acknowledgment

We thank financial support from Ministerio de Educación y Ciencia under project HOPE CSD2007-00007 (Consolider-Ingenio 2010).

References

- [1] C.J. Brabec, N.S. Sariciftci, C. Hummelen, *Adv. Mater.* 11 (2001) 15–26.
- [2] C. Lungenschmied, G. Dennier, H. Neugebauer, N.S. Sariciftci, E. Ehrenfreund, *Appl. Phys. Lett.* 89 (2006) 223519.

- [3] L.J.A. Koster, E.C.P. Smits, V.D. Mihailetschi, P.W.M. Blom, *Phys. Rev. B* 72 (2005) 085205.
- [4] P.W.M. Blom, V.D. Mihailetschi, L.J.A. Koster, D.E. Markov, *Adv. Mater.* 19 (2007) 1551–1566.
- [5] W. Ma, C. Yang, X. Gong, K.-S. Lee, A.J. Heeger, *Adv. Funct. Mater.* 15 (2005) 1617–1622.
- [6] C. Tanase, E.J. Meijer, P.W.M. Blom, D.M. de Leeuw, *Phys. Rev. Lett.* 91 (2003) 216601.
- [7] M.S.A. Abdou, F.P. Orfino, Y. Son, S. Holdcroft, *J. Am. Chem. Soc.* 119 (1997) 4518.
- [8] S. Hoshino, M. Yoshida, S. Uemura, T. Kodzasa, N. Takada, T. Kamata, K. Yase, *J. Appl. Phys.* 95 (2004) 5088.
- [9] J. Bisquert, *Phys. Chem. Chem. Phys.* 5 (2003) 5360.
- [10] I. Mora-Seró, J. Bisquert, F. Fabregat-Santiago, G. Garcia-Belmonte, G. Zoppi, K. Durose, Y. Proskuryakov, I. Oja, A. Belaidi, T. Dittrich, R. Tena-Zaera, A. Katty, C. Lévy-Clement, V. Barrioz, S.J.C. Irvine, *Nano Lett.* 6 (2006) 640.
- [11] I. Mora-Seró, Y. Luo, G. Garcia-Belmonte, J. Bisquert, D. Muñoz, C. Voz, J. Puigdollers, R. Alcobilla, *Sol. Energy Mater. Sol. Cells* 92 (2008) 505–509.
- [12] F. Fabregat-Santiago, J. Bisquert, G. Garcia-Belmonte, G. Boschloo, A. Hagfeldt, *Sol. Energy Mater. Sol. Cells* 87 (2005) 117–131.
- [13] Q. Wang, S. Ito, M. Grätzel, F. Fabregat-Santiago, I. Mora-Seró, J. Bisquert, T. Bosshoa, H. Imaic, *J. Phys. Chem. B* 110 (2006) 19406.
- [14] Q. Wang, J.-E. Moser, M. Grätzel, *J. Phys. Chem. B* 109 (2005) 14945.
- [15] J. Bisquert, A. Zaban, M. Greenshtein, I. Mora-Seró, *J. Am. Chem. Soc.* 126 (2004) 13550.
- [16] G. Dennler, C. Lungenschmied, N.S. Saricifti, R. Schwödiauer, S. Bauer, H. Reiss, *Appl. Phys. Lett.* 87 (2005) 163501.
- [17] M. Glatthaar, N. Mingirulli, B. Zimmermann, T. Ziegel, R. Kern, M. Niggemann, A. Hinsch, A. Gombert, *Phys. Stat. Sol. (a)* 202 (2005) R125–R127.
- [18] E.H. Rhoderick, R.H. Williams, *Metal-Semiconductor Contacts*, Clarendon Press, Oxford, 1988.
- [19] S.M. Sze, *Physics of Semiconductor Devices*, John Wiley and Sons, New York, 1981.
- [20] J. Bisquert, D. Cahen, G. Hodes, S. Rühle, A. Zaban, *J. Phys. Chem. B* 108 (2004) 8106–8118.
- [21] M.A. Green, J. Shewchun, *Solid State Electron.* 16 (1973) 1141–1150.
- [22] M. Glatthaar, M. Riede, N. Keegan, K. Sylvester-Hvid, B. Zimmermann, M. Niggemann, A. Hinsch, A. Gombert, *Sol. Energy Mater. Sol. Cells* 91 (2007) 390–393.
- [23] J. Bisquert, *J. Phys. Chem. B* 106 (2002) 325–333.
- [24] A. Pitarch, G. Garcia-Belmonte, I. Mora-Seró, J. Bisquert, *Phys. Chem. Chem. Phys.* 6 (2004) 2983–2988.
- [25] G. Garcia-Belmonte, J. Bisquert, G. Popkurov, *Appl. Phys. Lett.* 83 (2003) 2178–2180.
- [26] J. Bisquert, *Phys. Chem. Chem. Phys.* 10 (2008), doi:10.1039/b719943k.
- [27] V.D. Mihailetschi, J.K.J. van Duren, P.W.M. Blom, J.C. Hummelen, R.A.J. Janssen, J.M. Kroon, M.T. Rispens, W.J.H. Verhees, M.M. Wienk, *Adv. Funct. Mater.* 13 (2003) 43–46.
- [28] C. Arndt, U. Zhokhavets, M. Mohr, G. Gobsch, M. Al-Ibrahim, S. Sensfuss, *Synthetic Metals* 147 (2004) 257–260.
- [29] G. Dennler, A.J. Mozer, G. Juska, A. Pivrikas, R. Österbacka, A. Fuchsbaauer, N.S. Saricifti, *Organic Electron.* 7 (2006) 229–234.